

Efficient Multi-task Feature and Relationship Learning

Han Zhao

HAN.ZHAO@CS.CMU.EDU

Otilia Stretcu

OSTRETCU@CS.CMU.EDU

Renato Negrinho

NEGRINHO@CS.CMU.EDU

Alex Smola

ALEX@SMOLA.ORG

Geoff Gordon

GGORDON@CS.CMU.EDU

Machine Learning Department, Carnegie Mellon University, Pittsburgh, PA, USA

Abstract

In this paper we propose a multi-convex framework for multi-task learning that improves predictions by learning relationships both between tasks and between features. Our framework is a generalization of related methods in multi-task learning, that either learn task relationships, or feature relationships, but not both. We start with a hierarchical Bayesian model, and use the empirical Bayes method to transform the underlying inference problem into a multi-convex optimization problem. We propose a coordinate-wise minimization algorithm that has a closed form solution for each block subproblem. Naively these solutions would be expensive to compute, but by using the theory of doubly stochastic matrices, we are able to reduce the underlying matrix optimization subproblem into a minimum weight perfect matching problem on a complete bipartite graph, and solve it analytically and efficiently. To solve the weight learning subproblem, we propose three different strategies, including a gradient descent method with linear convergence guarantee when the instances are not shared by multiple tasks, and a numerical solution based on Sylvester equation when instances are shared. We demonstrate the efficiency of our method on both synthetic datasets and real-world datasets. Experiments show that the proposed optimization method is orders of magnitude faster than an off-the-shelf projected gradient method, and our model is able to exploit the correlation structures among multiple tasks and features.

1. Introduction

Multi-task learning has received considerable interest in the past decades (Caruana, 1997; Evgeniou and Pontil, 2004; Argyriou et al., 2007, 2008; Kato et al., 2008; Liu et al., 2009; Zhang and Yeung, 2010a; Zhang and Schneider, 2010; Li et al., 2015). One of the underlying assumptions behind many multi-task learning algorithms is that the tasks are related to each other. Hence, a key question is how to define the notion of task relatedness, and how to capture it in the learning formulation. A common assumption is that tasks can be described by weight vectors, either from finite dimensional space or Reproducing Kernel Hilbert Space (RKHS), and that they are sampled from a shared prior distribution over their space (Liu et al., 2009; Zhang and Yeung, 2010a,b). Another strand of work assumes common feature representations to be shared among multiple tasks, and the goal is to learn the shared representation as well as task-specific parameters simultaneously (Thrun, 1996a; Caruana, 1997; Evgeniou and Pontil, 2007; Argyriou et al., 2008). Moreover, when structure about multiple tasks is available, e.g., task-specific descriptors (Bonilla et al., 2007a) or a task similarity graph (Evgeniou and Pontil, 2004), regularizers can often be incorporated into the learning formulation to explicitly penalize hypotheses that are not consistent with the given structure.

In this paper we follow the first line of work and propose a multi-convex framework for multi-task learning. Our method improves predictions over tabula rasa learning by assuming that all the task

vectors are sampled from a common, shared prior. There have been several attempts to improve predictions along this direction by either learning the relationships between different tasks (Zhang and Yeung, 2010a), known as *Multi-Task Relationship Learning* (MTRL), or by exploiting the relationships between different features (Argyriou et al., 2008), which is known as *Multi-Task Feature Learning* (MTFL). Zhang and Schneider (2010) proposed a multi-task learning framework where both the task and feature relationships are inferred from data by assuming a sparse matrix-normal penalty on both the task and feature representations. As in that paper, our multi-task learning framework is a generalization of both MTRL and MTFL, which learns the relationships both between tasks and between features simultaneously. This property is favorable for applications where we not only aim for better generalization, but also seek to have a clear understanding about the relationships among different tasks. Compared to the sparse regularization approach in Zhang and Schneider (2010), our framework is free of the sparsity assumption, and as a result, it admits an efficient optimization scheme where we are able to derive analytic solutions to each subproblem, whereas in (Zhang and Schneider, 2010) iterative methods have to be used for each subproblem. We term our proposed framework *FEature and Task Relationship learning* (FETR). Our main contributions are summarized as follows:

- First, we formulate FETR as a hierarchical Bayes model, where a carefully chosen prior is imposed on the task vectors in order to capture the relatedness between tasks and features at the same time. Our model is free of sparsity assumption that was usually made in the literature to make the algorithm scalable. We apply an empirical Bayes (Carlin and Louis, 1997) method to approximate the exact posterior distribution, leading to a learning formulation where the goal is to optimize over both the model parameters, i.e., the task vectors, as well as two covariance matrices in the prior.
- Second, we transform the optimization problem in FETR into a multi-convex structure, and design an alternating direction algorithm using block coordinate-wise minimization to solve this problem efficiently. Specifically, we achieve this by reducing an underlying matrix optimization problem with positive definite constraints into a minimum weight perfect matching problem on a complete bipartite graph, where we are able to solve analytically using combinatorial techniques. To solve the weight learning subproblem, we propose three different strategies, including a closed form solution, a gradient descent method with linear convergence guarantee when the instances are not shared by multiple tasks, and a numerical solution based on Sylvester equation when instances are shared.
- Next, we demonstrate the efficiency of the proposed optimization algorithm by comparing it with an off-the-shelf projected gradient descent algorithm on synthetic data. Experiments show that the proposed optimization method is orders of magnitude faster than its competitor, and it often converges to a better local solution.
- Lastly, we test the statistical performance of FETR on modeling real-world related tasks by comparing it with single task learning, as well as MTFL and MTRL. Results show that FETR is not only able to give better predictions, but can also effectively exploit the correlation structures among multiple tasks. We also study FETR and its relationship with existing multi-task learning algorithms, including MTFL and MTRL, in a general regularization framework, showing that some of them can be viewed as special cases of FETR.

2. Multi-task Feature and Relationship Learning

2.1 Notation and Setup

We use \mathbb{S}_+^m and \mathbb{S}_{++}^m to denote the m -dimensional symmetric positive semidefinite cone and m -dimensional symmetric positive definite cone, respectively. We write $\text{tr}(A)$ for the trace of a matrix A . Finally, we use $G = (A, B, E, w)$ to denote a weighted bipartite graph with vertex sets A, B , edge set E , and weight function $w : E \rightarrow \mathbb{R}_+$. $[d]$ denotes the set $\{1, 2, \dots, d\}$.

We consider the following setup. Suppose we are given m learning tasks $\{T_i\}_{i=1}^m$, where for each learning task T_i we have access to a training set \mathcal{D}_i with n_i data instances $(\mathbf{x}_i^j, y_i^j), j \in [n_i]$. Here we focus on the supervised learning setting where $\mathbf{x}_i^j \in \mathcal{X}_i \subseteq \mathbb{R}^d$ and $y_i^j \in \mathcal{Y}_i$, where $\mathcal{Y}_i = \mathbb{R}$ for a regression problem and $\mathcal{Y}_i = \{1, -1\}$ for a binary classification problem. Let $f_i(\mathbf{w}_i, \cdot) : \mathcal{X}_i \rightarrow \mathcal{Y}_i$ be our predictor/model with parameter \mathbf{w}_i and $\ell(\cdot, \cdot) : \mathcal{Y}_i \times \mathcal{Y}_i \rightarrow \mathbb{R}_+$ be the loss function for task T_i . For ease of discussion, in what follows, we will assume our model for each task T_i to be a linear regression, i.e., $f_i(\mathbf{w}_i, \mathbf{x}) = \mathbf{w}_i^T \mathbf{x}$. Our approach can also be translated into a classification problem, e.g., logistic regression, linear SVM, etc. We refer interested readers to the appendix for proofs of claims and theorems in the paper.

2.2 Hierarchical Bayes model

Based on the linear regression model, the likelihood function for task i is given by:

$$y_i^j \mid \mathbf{x}_i^j, \mathbf{w}_i, \epsilon_i \sim \mathcal{N}(\mathbf{w}_i^T \mathbf{x}_i^j, \epsilon_i^2) \quad (1)$$

where $\mathcal{N}(\mathbf{m}, \Sigma)$ is the multivariate normal distribution with mean \mathbf{m} and covariance matrix Σ . Let $W = (\mathbf{w}_1, \dots, \mathbf{w}_m) \in \mathbb{R}^{d \times m}$ be the model parameter (regression weights) for m different tasks. Applying a hierarchical Bayes approach, we specify a prior distribution over the model parameter W . Specifically, we define the prior distribution over W to be

$$W \mid \xi, \Omega_1, \Omega_2 \sim \left(\prod_{i=1}^m \mathcal{N}(\mathbf{w}_i \mid \mathbf{0}, \xi_i \mathbf{I}_d) \right) q(W \mid \Omega_1, \Omega_2) \quad (2)$$

where \mathbf{I}_d is a $d \times d$ identity matrix and $\mathbf{0} \in \mathbb{R}^d$ is a d -dimensional vector of all 0s. The form of $q(W \mid \Omega_1, \Omega_2)$ is given by

$$q(W \mid \Omega_1, \Omega_2) = \mathcal{MN}_{d \times m}(W \mid \mathbf{0}_{d \times m}, \Omega_1, \Omega_2)$$

where $\mathcal{MN}_{d \times m}(M, A, B)$ denotes a matrix-variate normal distribution (Gupta and Nagar, 1999) with mean $M \in \mathbb{R}^{d \times m}$, row covariance matrix $A \in \mathbb{S}_{++}^d$ and column covariance matrix $B \in \mathbb{S}_{++}^m$.¹ As we will see later, the first term in the RHS of Eq. 2 can be interpreted as a regularizer to penalize the model complexity of f_i and $q(W \mid \Omega_1, \Omega_2)$ encodes the structure about the task vectors W . Intuitively, by imposing structure on the row covariance and column covariance matrices, we can incorporate our prior knowledge about the correlation among features as well as the relationship among different tasks. It is worth pointing out that one can specify other forms of prior distributions instead of (2), as in (Liu et al., 2009) and (Zhang and Yeung, 2010b) where the authors use a Laplacian prior and a generalized t process, respectively. As we will see shortly, the advantage of

1. The probability density function is $p(X \mid M, A, B) = \frac{\exp(-\frac{1}{2} \text{tr}(A^{-1}(X-M)B^{-1}(X-M)^T))}{(2\pi)^{md/2} |A|^{m/2} |B|^{d/2}}$.

using the specific prior in Eq. 2 is that, when applying an empirical Bayes approach to solve our model, we will explicitly have access to the optimal covariance matrices Ω_1 and Ω_2 over the row vectors and column vectors of W .

2.3 Empirical Bayes method

Given the prior distribution over W and the likelihood function as specified in Eq. 2 and Eq. 1, the posterior distribution of the model parameter W is given by

$$p(W | X, \mathbf{y}) \propto p(W)p(\mathbf{y} | X, W) \quad (3)$$

A standard Bayesian inference approach applied here would be to specify another prior distribution $p(\Omega_1, \Omega_2)$ over both covariance matrices Ω_1 and Ω_2 and then compute the above exact posterior distribution as follows:

$$p(W | X, \mathbf{y}) \propto p(W)p(\mathbf{y} | X, W) = p(\mathbf{y} | X, W) \int p(W | \Omega_1, \Omega_2)p(\Omega_1, \Omega_2) d\Omega_1 d\Omega_2$$

This is computationally intractable in our case, since we do not have an analytic form for the posterior distribution. So instead of computing the integration exactly, we take an empirical Bayes approach: we approximate the intractable integration above by

$$p(W | X, \mathbf{y}) \approx \max_{\Omega_1, \Omega_2} p(\mathbf{y} | X, W)p(W | \Omega_1, \Omega_2) \quad (4)$$

The underlying assumption behind this approximation is that when the exact posterior distribution is sharply concentrated, the integral for the marginal $p(W) = \int p(W | \Omega_1, \Omega_2)p(\Omega_1, \Omega_2) d\Omega_1 d\Omega_2$ may be not much changed by replacing the prior distribution over Ω_1 and Ω_2 with a point estimate representing the peak of the distribution.

Substituting Eq. 2 and Eq. 1 into Eq. 4 and omitting the constant terms which do not depend on W , Ω_1 and Ω_2 , we maximize the approximate posterior distribution by optimizing over W , Ω_1 and Ω_2 , leading us to the following optimization scheme:

$$\begin{aligned} \underset{W, \Omega_1, \Omega_2}{\text{minimize}} \quad & \sum_{i=1}^m \frac{1}{\xi_i^2} \mathbf{w}_i^T \mathbf{w}_i + m \log |\Omega_1| + d \log |\Omega_2| + \\ & \sum_{i=1}^m \frac{1}{\epsilon_i^2} \sum_{j=1}^{n_i} (y_i^j - \mathbf{w}_i^T \mathbf{x}_i^j)^2 + \text{tr}(\Omega_1^{-1} W \Omega_2^{-1} W^T) \\ \text{subject to} \quad & \Omega_1 \succ 0, \Omega_2 \succ 0 \end{aligned} \quad (5)$$

It is worth pointing out here the optimal value of (5) may not be achieved since the constraint set is open. In fact, we can always decrease the objective function by setting $W = \mathbf{0}_{d \times m}$ and make the eigenvalues of both Ω_1 and Ω_2 infinitely close to 0 but strictly greater than 0. In this case, the value of $m \log |\Omega_1|$ and $d \log |\Omega_2|$ will approach $-\infty$ hence (5) has no lower bound. We will fix this technical issue in the next section by imposing boundedness constraints on both Ω_1 and Ω_2 .

For simplicity of later discussion, we will assume that $\xi_i = \xi$ and $\epsilon_i = \epsilon$, $\forall i \in [m]$. Before discussing the details on how to efficiently solve the above optimization program, let us inspect the equation and discuss several of its special cases. If we fix $\Omega_1 = \mathbf{I}_d$ and $\Omega_2 = \mathbf{I}_m$, the above

optimization problem can be decomposed into m independent single task learning problems, where each task corresponds to a ridge regression problem. More generally, block diagonal designs of the covariance matrices Ω_1 and Ω_2 will exhibit group/clustering properties of the features or tasks. On the other hand, when $m = 1$, i.e., in the single task learning setting, and we fix Ω_1 and Ω_2 manually, then the above optimization problem reduces to linear regression with a weighted linear smoother, where the smoother is specified by $\lambda \mathbf{I}_d + \Omega_1^{-1}$. An optimal solution can be obtained in closed form. In this case Ω_1^{-1} plays the role of a stabilizer and reweights the relative importance of different features. Similarly, Ω_2^{-1} models the correlation between different tasks and their relative strength.

3. Multi-convex Optimization

Although the empirical Bayes framework is appealing, the optimization posed in (5) is not easy to solve directly. In this section we first show that (5) can be converted into a multi-convex optimization problem. A multi-convex function is a generalization of a bi-convex function (Gorski et al., 2007) into multiple variables or blocks of variables.

Definition 3.1 (Multi-convex function (Xu and Yin, 2013)). A function $g(\mathbf{x}_1, \dots, \mathbf{x}_k)$ is called *multi-convex* if for each block of variables \mathbf{x}_i , g is a convex function of \mathbf{x}_i while keeping all the other blocks of variables fixed.

3.1 Multi-convex Formulation

It is not hard to see that the optimization problem in (5) is not convex since $m \log |\Omega_1| + d \log |\Omega_2|$ is a concave function of Ω_1 and Ω_2 (Boyd and Vandenberghe, 2004). Also, (5) is unbounded from below as we analyzed in the last section. To handle these technical issues, we introduce a boundedness constraint into the constraint set of Ω_1 and Ω_2 . More concretely, instead of constraining $\Omega_1 \succ 0$ and $\Omega_2 \succ 0$, we make $\frac{1}{u} \mathbf{I}_d \preceq \Omega_1 \preceq \frac{1}{l} \mathbf{I}_d$ and $\frac{1}{u} \mathbf{I}_m \preceq \Omega_2 \preceq \frac{1}{l} \mathbf{I}_m$, where $u > l > 0$ are constants. One can understand this constraint as putting an implicit uniform prior distribution $p(\Omega_1, \Omega_2)$ over the set specified by the constraint. Technically, the boundedness constraint make the feasible sets for Ω_1 and Ω_2 compact, hence by the extreme value theorem minimum is guaranteed to be achieved since the objective function is continuous.

Next, we apply a well known transformation to both Ω_1 and Ω_2 so that the new optimization problem is multi-convex in terms of the transformed variables. We define $\Sigma_1 \triangleq \Omega_1^{-1}$ and $\Sigma_2 \triangleq \Omega_2^{-1}$. Both Σ_1 and Σ_2 are well-defined because Ω_1 and Ω_2 are constrained to be positive definite matrices. The transformed optimization formulation based on W, Σ_1 and Σ_2 is

$$\begin{aligned}
 & \underset{W, \Sigma_1, \Sigma_2}{\text{minimize}} && \sum_{i=1}^m \sum_{j=1}^{n_i} (y_i^j - \mathbf{w}_i^T \mathbf{x}_i^j)^2 + \eta \sum_{i=1}^m \mathbf{w}_i^T \mathbf{w}_i \\
 & && - \rho(m \log |\Sigma_1| + d \log |\Sigma_2|) \\
 & && + \rho \text{tr}(\Sigma_1 W \Sigma_2 W^T) \\
 & \text{subject to} && l \mathbf{I}_d \preceq \Sigma_1 \preceq u \mathbf{I}_d, l \mathbf{I}_m \preceq \Sigma_2 \preceq u \mathbf{I}_m
 \end{aligned} \tag{6}$$

where we define $\eta = (\epsilon/\xi)^2$ and $\rho = \epsilon^2$ to simplify the notation.

Claim 3.1. The objective function in (6) is multi-convex.

3.2 Block Coordinate Minimization

Based on the multi-convex formulation developed in the last section, we propose an alternating direction algorithm using block coordinate-wise minimization to optimize the objective given in (6). In each iteration k we alternatively minimize over W with Σ_1 and Σ_2 fixed, then minimize over Σ_1 with W and Σ_2 fixed, and lastly minimize Σ_2 with W and Σ_1 fixed. The whole procedure is repeated until a stationary point is found or the decrease in the objective function is less than a pre-specified threshold. In what follows, we assume $n = n_i, \forall i \in [m]$ to simplify the notation. Let $Y = (\mathbf{y}_1, \dots, \mathbf{y}_m) \in \mathbb{R}^{n \times m}$ be the labeling matrix and $X \in \mathbb{R}^{n \times d}$ be the feature matrix shared by all the tasks. Using this notation, the objective function can be equivalently expressed in matrix form as:

$$\begin{aligned} & \underset{W, \Sigma_1, \Sigma_2}{\text{minimize}} \quad \|Y - XW\|_F^2 + \eta \|W\|_F^2 + \rho \|\Sigma_1^{1/2} W \Sigma_2^{1/2}\|_F^2 \\ & \quad - \rho(m \log |\Sigma_1| + d \log |\Sigma_2|) \\ & \text{subject to} \quad lI_d \preceq \Sigma_1 \preceq uI_d, lI_m \preceq \Sigma_2 \preceq uI_m \end{aligned} \quad (7)$$

There are lots of ways to try to solve the above, and we discuss next how to do so efficiently.

3.2.1 OPTIMIZATION W.R.T W

In order to minimize over W when both Σ_1 and Σ_2 are fixed, we solve the following subproblem:

$$\underset{W}{\text{minimize}} \quad h(W) \triangleq \|Y - XW\|_F^2 + \eta \|W\|_F^2 + \rho \|\Sigma_1^{1/2} W \Sigma_2^{1/2}\|_F^2 \quad (8)$$

As shown in the last section, this is an unconstrained convex optimization problem. We present three different algorithms to find the optimal solution of this subproblem. The first one guarantees to find an exact solution in closed form in $O(m^3 d^3)$ time, by using the isomorphism between $\mathbb{R}^{d \times m}$ and \mathbb{R}^{dm} . The second one does gradient descent with fixed step size to iteratively refine the solution, and we show that in our case a linear convergence speed can be guaranteed. The third one finds the optimal solution by solving the Sylvester equation (Bartels and Stewart, 1972) characterized by the first-order optimality condition, after a proper transformation.

A closed form solution. It is worth noting that it is not obvious how to obtain a closed form solution directly from the formulation in (8). An application of the first order optimality condition to (8) will lead to the following equation:

$$(X^T X + \eta I_d)W + \rho \Sigma_1 W \Sigma_2 = X^T Y \quad (9)$$

Except for the special case where $\Sigma_2 = cI_m$ with $c > 0$ a constant, the above equation does not admit an easy closed form solution in its matrix representation. The workaround is based on the fact that $\mathbb{R}^{d \times m} \simeq \mathbb{R}^{dm}$, i.e., the $d \times m$ dimensional matrix space is isomorphic to the dm dimensional vector space, with the $\text{vec}(\cdot)$ operator implementing the isomorphism from $\mathbb{R}^{d \times m}$ to \mathbb{R}^{dm} . Using this property, we claim

Claim 3.2. (8) can be solved in closed form in $O(m^3 d^3 + mnd^2)$ time; the optimal $\text{vec}(W^*)$ has the following form:

$$(I_m \otimes (X^T X) + \eta I_{md} + \rho \Sigma_2 \otimes \Sigma_1)^{-1} \text{vec}(X^T Y) \quad (10)$$

W^* can then be obtained simply by reformatting $\text{vec}(W^*)$ into a $d \times m$ matrix. The computational bottleneck in the above procedure is in solving an $md \times md$ system of equations, which scales as $O(m^3d^3)$ if no further sparsity structure is available. The overall computational complexity is $O(m^3d^3 + mnd^2)$.

Gradient descent. The closed form solution shown above scales cubically in both m and d , and requires us to explicitly form a matrix of size $md \times md$. This can be intractable even for moderate m and d . In such cases, instead of computing an exact solution to (8), we can use gradient descent with fixed step size to obtain an approximate solution.

The objective function $h(W)$ in (8) is differentiable and its gradient can be obtained in $O(m^2d + md^2)$ time as follows:

$$\nabla_W h(W) = X^T(Y - XW) + \eta W + \rho \Sigma_1 W \Sigma_2 \quad (11)$$

Note that we can compute in advance both $X^T Y$ and $X^T X$ in $O(nd^2)$ time, and cache them so that we do not need to recompute them in each gradient update step. Let $\lambda_i(A)$ be the i th largest eigenvalue of a real symmetric matrix A . We provide a linear convergence guarantee for the gradient method in Thm. 3.1. Our proof technique is adapted from Nesterov (2013) where we extend it to matrix function.

Theorem 3.1. Let $\lambda_l = \lambda_d(X^T X) + \eta + \rho l^2$, $\lambda_u = \lambda_1(X^T X) + \eta + \rho u^2$ and $\gamma = (\frac{\lambda_u - \lambda_l}{\lambda_u + \lambda_l})^2$. Choose $0 < t \leq 2/(\lambda_u + \lambda_l)$. For all $\varepsilon > 0$, gradient descent with step size t converges to the optimal solution within $O(\log_{1/\gamma}(1/\varepsilon))$ steps.

Remark. The computational complexity to achieve an ε approximate solution using gradient descent is $O(nd^2 + \log_{1/\gamma}(1/\varepsilon)(m^2d + md^2))$. Compared with the $O(m^3d^3 + mnd^2)$ complexity for the exact solution, the gradient descent algorithm scales much better provided $\gamma \ll 1$, i.e., the condition number $\kappa \triangleq \lambda_u/\lambda_l$ is not too large. As a side note, when the condition number is large, we can effectively reduce it to \sqrt{k} by using conjugate gradient method (Shewchuk et al., 1994).

Sylvester equation. In the field of control theory, a Sylvester equation (Bhatia and Rosenthal, 1997) is a matrix equation of the form $AX + XB = C$, where the goal is to find a solution matrix X given A, B and C . For this problem, there are efficient numerical algorithms with highly optimized implementations that can obtain a solution within cubic time. For example, the Bartels-Stewart algorithm (Bartels and Stewart, 1972) solves the Sylvester equation by first transforming A and B into Schur forms by QR factorization, and then solves the resulting triangular system via back-substitution. Our third approach is based on the observation that we can equivalently transform the first-order optimality equation given in (9) into a Sylvester equation by multiplying Σ_1^{-1} at both sides of the equation:

$$\Sigma_1^{-1}(X^T X + \eta I_d)W + W(\rho \Sigma_2) = \Sigma_1^{-1}X^T Y \quad (12)$$

Then finding the optimal solution of the subproblem amounts to solving the above Sylvester equation. Specifically, the solution to the above equation can be obtained using the Bartels-Stewart algorithm within $O(m^3 + d^3 + nd^2)$.

Both the gradient descent and the Bartels-Stewart algorithm find the optimal solution in cubic time. However, the gradient descent algorithm is more widely applicable than the Bartels-Stewart algorithm: the Bartels-Stewart algorithm only applies to the case where all the tasks share the same

instances, so that we can write down the matrix equation explicitly, while gradient descent can be applied in the case where each task has different number of inputs and those inputs are not shared among tasks. On the other hand, as we will see shortly in the experiments, in practice the Bartels-Stewart algorithm is faster than gradient descent, and provides a more numerically stable solution.

3.2.2 OPTIMIZATION W.R.T. Σ_1 AND Σ_2

Before we delve into the detailed analysis below, we first list the final algorithms used to optimize Σ_1 and Σ_2 in Alg. 1 and Alg. 2, respectively. They are remarkably simple: each algorithm only involves one SVD, one truncation and two matrix multiplications. The computational complexity of Alg. 1 (Alg. 2) is bounded by $O(m^2d + md^2 + d^3)$ ($O(m^2d + md^2 + m^3)$).

Algorithm 1 Minimize Σ_1

Input: W, Σ_2 and l, u .
 1: $[V, \nu] \leftarrow \text{SVD}(W\Sigma_2W^T)$.
 2: $\lambda \leftarrow \mathbb{T}_{[l,u]}(m/\nu)$.
 3: $\Sigma_1 \leftarrow V\text{diag}(\lambda)V^T$.

Algorithm 2 Minimize Σ_2

Input: W, Σ_1 and l, u .
 1: $[V, \nu] \leftarrow \text{SVD}(W^T\Sigma_1W)$.
 2: $\lambda \leftarrow \mathbb{T}_{[l,u]}(d/\nu)$.
 3: $\Sigma_2 \leftarrow V\text{diag}(\lambda)V^T$.

We focus on analyzing the optimization w.r.t. Σ_1 . A similar analysis applies to Σ_2 . In order to minimize over Σ_1 when W and Σ_2 are fixed, we solve the following subproblem:

$$\begin{aligned} & \underset{\Sigma_1}{\text{minimize}} && \text{tr}(\Sigma_1 W \Sigma_2 W^T) - m \log |\Sigma_1| \\ & \text{subject to} && lI_d \preceq \Sigma_1 \preceq uI_d \end{aligned} \tag{13}$$

Although (13) is a convex optimization problem, it is computationally expensive to solve using off-the-shelf algorithms because of the constraints as well as the nonlinearity of the objective function. Surprisingly, we can find a closed form optimal solution to this problem as well, using tools from the theory of doubly stochastic matrices (Dufossé and Uçar, 2016) and perfect bipartite graph matching. Since $\Sigma_2 \in \mathbb{S}_{++}^m$, it follows that $W\Sigma_2W^T \in \mathbb{S}_+^d$. Without loss of generality, we can reparametrize $\Sigma_1 = U\Lambda U^T$, where $\Lambda = \text{diag}(\lambda_1, \dots, \lambda_d)$ with $u \geq \lambda_1 \geq \lambda_2 \geq \dots \geq \lambda_d \geq l$ and $U \in \mathbb{R}^{d \times d}$ with $U^T U = U U^T = I_d$ using spectral decomposition. Similarly, we can represent $W\Sigma_2W^T = VNV^T$ where $V \in \mathbb{R}^{d \times d}$, $V^T V = V V^T = I_d$ and $N = \text{diag}(\nu_1, \dots, \nu_d)$ with $0 \leq \nu_1 \leq \dots \leq \nu_d$. Note that the eigenvectors in N corresponds to eigenvalues in increasing order rather than decreasing order, for reasons that will become clear below.

Using the new representation and realizing that U is an orthonormal matrix, we have

$$\log |\Sigma_1| = \log |U\Lambda U^T| = \log |\Lambda| \tag{14}$$

and

$$\text{tr}(\Sigma_1 W \Sigma_2 W^T) = \text{tr}(\Lambda U^T V N V^T U) \tag{15}$$

Set $K = U^T V$. Since both U and V are orthonormal matrices, K is also an orthonormal matrix. We can further transform (15) to be

$$\text{tr}(\Lambda U^T V N V^T U) = \text{tr}((\Lambda K)(KN)^T)$$

Note that the mapping between U and K is bijective since V is a fixed orthonormal matrix. Using K and Λ , we can equivalently transform the optimization problem (13) into the following new form:

$$\begin{aligned} & \underset{K, \Lambda}{\text{minimize}} && -m \log |\Lambda| + \text{tr}((\Lambda K)(KN)^T) \\ & \text{subject to} && l \text{diag}(\mathbf{1}_d) \leq \Lambda \leq u \text{diag}(\mathbf{1}_d) \\ & && K^T K = K K^T = I_d \end{aligned} \quad (16)$$

where $\mathbf{1}_d$ is a d -dimensional vector of all ones. At first glance it seems that the new form of optimization is more complicated to solve since it is even not a convex problem due to the quadratic equality constraint. However, as we will see shortly, the new form helps to decouple the interaction between K and Λ in that K does not influence the first term $-m \log |\Lambda|$. This implies that we can first partially optimize over K , finding the optimal solution as a function of Λ , and then optimize over Λ . Mathematically, it means:

$$\min_{K, \Lambda} -m \log |\Lambda| + \text{tr}((\Lambda K)(KN)^T) \Leftrightarrow \min_{\Lambda} -m \log |\Lambda| + \min_K \text{tr}((\Lambda K)(KN)^T) \quad (17)$$

Consider the minimization over K :

$$\text{tr}((\Lambda K)(KN)^T) = \sum_{i=1}^d \sum_{j=1}^d \lambda_i K_{ij}^2 \nu_j = \lambda^T P \nu$$

where we define $P = K \circ K$, $\lambda = (\lambda_1, \dots, \lambda_d)^T$ and $\nu = (\nu_1, \dots, \nu_d)^T$. Since K is an orthonormal matrix, we have the following two equations: $\sum_{j=1}^d P_{ij} = \sum_{j=1}^d K_{ij}^2 = 1$, $\forall i \in [d]$, $\sum_{i=1}^d P_{ij} = \sum_{i=1}^d K_{ij}^2 = 1$, $\forall j \in [d]$, which implies that P is a doubly stochastic matrix (Dufossé and Uçar, 2016). The partial minimization over K can be equivalently solved by the partial minimization over P :

$$\min_K \text{tr}((\Lambda K)(KN)^T) = \min_P \lambda^T P \nu \quad (18)$$

In order to solve the minimization over the doubly stochastic matrix P , we need to introduce the following theorems.

Theorem 3.2 (Optimality of extreme points (Bertsimas and Tsitsiklis, 1997)). Consider the minimization of a linear programming problem over a polyhedron P . Suppose that P has at least one extreme point and that there exists an optimal solution. Then there exists an optimal solution which is an extreme point of P .

Definition 3.2 (Birkhoff polytope). The *Birkhoff polytope* B_d is the set of $d \times d$ doubly stochastic matrices. B_d is a convex polytope.

Theorem 3.3 (Birkhoff-von Neumann theorem). Let B_d be the Birkhoff polytope. B_d is the convex hull of the set of $d \times d$ permutation matrices. Furthermore, the vertices (extreme points) of B_d are the permutation matrices.

The following lemma follows immediately from the above two theorems:

Lemma 3.1. There exists an optimal solution P to the optimization problem (18) that is a $d \times d$ permutation matrix.

Given that there exists an optimal solution that is a permutation matrix, we can reduce (18) into a minimum-weight perfect matching problem on a complete bipartite graph. The problem of minimum-weight perfect matching is defined as follows.

Definition 3.3 (Minimum-weight perfect matching). Let $G = (V, E)$ be an undirected graph with edge weight $w : E \rightarrow \mathbb{R}_+$. A *matching* in G is a set $M \subseteq E$ such that no two edges in M have a vertex in common. A matching M is called *perfect* if every vertex from V occurs as the endpoint of some edge in M . The weight of a matching M is $w(M) = \sum_{e \in M} w(e)$. A matching M is called a *minimum-weight perfect matching* if it is a perfect matching that has the minimum weight among all the perfect matchings of G .

For any $\lambda, \nu \in \mathbb{R}_+^d$, we can construct a weighted $d - d$ bipartite graph $G = (V_\lambda, V_\nu, E, w)$ as follows:

- For each λ_i , construct a vertex $v_{\lambda_i} \in V_\lambda, \forall i$.
- For each ν_j , construct a vertex $v_{\nu_j} \in V_\nu, \forall j$.
- For each pair $(v_{\lambda_i}, v_{\nu_j})$, construct an edge $e(v_{\lambda_i}, v_{\nu_j}) \in E$ with edge weight $w(e(v_{\lambda_i}, v_{\nu_j})) = \lambda_i \nu_j$.

Theorem 3.4. The minimum value of (18) is equal to the minimum weight of a perfect matching on $G = (V_\lambda, V_\nu, E, w)$. Furthermore, the optimal solution P of (18) can be constructed from the minimum-weight perfect matching M on G .

We do not even need to run standard graph matching algorithms to solve our matching problem. Instead, Thm. 3.5 gives a closed form solution.

Theorem 3.5. Let $\lambda = (\lambda_1, \dots, \lambda_d)$ and $\nu = (\nu_1, \dots, \nu_d)$ with $\lambda_1 \geq \dots \geq \lambda_d$ and $\nu_1 \leq \dots \leq \nu_d$. The minimum-weight perfect matching on G is $\pi^* = \{(v_{\lambda_i}, v_{\nu_i}) : 1 \leq i \leq d\}$ with the minimum weight $w(\pi^*) = \sum_{i=1}^d \lambda_i \nu_i$.

The permutation matrix that achieves the minimum weight is $P^* = I_d$ since $\pi^*(\lambda_i) = \nu_i$. Note that $P = K \circ K$, it follows that the optimal K^* is also I_d . Hence we can solve for the optimal U^* matrix by solving the equation $U^{*T} V = I_d$, which leads to $U^* = V$.

Now plug in the optimal $K^* = I_d$ into (17). The optimization w.r.t. Λ decomposes into d independent optimization problems, each of which being a simple scalar optimization problem:

$$\begin{aligned} & \underset{\lambda}{\text{minimize}} && \sum_{i=1}^d \lambda_i \nu_i - m \log \lambda_i \\ & \text{subject to} && l \leq \lambda_i \leq u, \quad \forall i = 1, \dots, d \end{aligned} \tag{19}$$

Depending on whether the value m/ν_i is within the range $[l, u]$, the optimal solution λ_i^* for each scalar minimization problem may take different forms. Define a soft-thresholding operator $\mathbb{T}_{[l,u]}(x)$ as follows:

$$\mathbb{T}_{[l,u]}(z) = \begin{cases} l, & z < l \\ z, & l \leq z \leq u \\ u, & z > u \end{cases} \tag{20}$$

Using this soft-thresholding operator, we can express the optimal solution λ_i^* as $\lambda_i^* = \mathbb{T}_{[l,u]}(m/\nu_i)$. Combining all the analysis above, we get the algorithms listed at the beginning of this section to optimize Σ_1 (Alg. 1) and Σ_2 (Alg. 2).

4. Experiments

In this section we analyze the statistical performance of FETR as well as the efficiency of the proposed coordinate minimization algorithm for solving the underlying multi-convex optimization problem.

4.1 Convergence Analysis

We first investigate the efficiency and scalability of the three different algorithms for minimizing w.r.t. W on synthetic data sets. To this end, for each experiment, we generate a synthetic data set which consists of $n = 10^4$ instances that are shared among all the tasks. All the instances are randomly sampled uniformly from $[0, 1]^d$. We gradually increase the dimension of features, d , and the number of tasks, m to test scalability. The first algorithm implements the closed form solution (21) by explicitly computing the $md \times md$ tensor product matrix and then solving the linear system. The second one is the proposed gradient descent, whose stop condition is met when either the norm of the gradient is less than 0.01 or the algorithm has looped more than 50 iterations. The last one uses the Bartels-Stewart algorithm to solve the equivalent Sylvester equation to compute W . We use open source toolkit `scipy` whose backend implementation uses highly optimized Fortran code. For all the synthetic experiments we set $l = 0.01$ and $u = 100$, which corresponds to a condition number of 10^4 . We fix the coefficients $\eta = 1.0$ and $\rho = 1.0$ since they will not affect the convergence speed. The experimental results are shown in Fig. 1.

As expected, the closed form solution does not scale to problems of even moderate size due to its large memory requirement. In practice the Bartels-Stewart algorithm is about one order of magnitude faster than the gradient descent method when either m or d is large (hundreds of features or hundreds of tasks).

It is also worth pointing out here that the Bartels-Stewart algorithm is the most numerically stable algorithm among the three based on our observations. Hence in the following experiments where the Bartels-Stewart solver can be applied we will use it, while in the case where it cannot be applied, we will use the gradient descent method. We now compare our proposed coordinate minimization algorithm with an off-the-shelf projected gradient method to solve the optimization problem (7). Specifically, the projected gradient method updates W, Σ_1 and Σ_2 based on the gradient direction in each iteration and then projects Σ_1 and Σ_2 into the corresponding feasible regions. In this experiment we set the number of instances to be 10^4 , the dimension of feature vectors to be 10^4 and the number of tasks to be 10. All the instances are shared among all the tasks, so that the Sylvester solver is used to optimize W in coordinate minimization. We repeat the experiments 10 times and report the log function values versus the time used by these two algorithms; see Fig. 2. We use a desktop with twelve i7-6850K CPU cores to conduct this experiment. It is clear from this synthetic experiment that our proposed algorithm not only converges much faster than projected gradient descent, but also achieves better results.

4.2 Synthetic Toy Problem

Before we proceed to do experiments on real-world data sets, we generate a toy data set and conduct a synthetic experiment to show that the proposed model can indeed learn the relationships between task vectors and feature vectors simultaneously. We randomly generate 10 data points uniformly from the range $[0, 100]^2$. We consider the following three regression tasks: $y_1 = 10x_1 + 10x_2 + 10$,

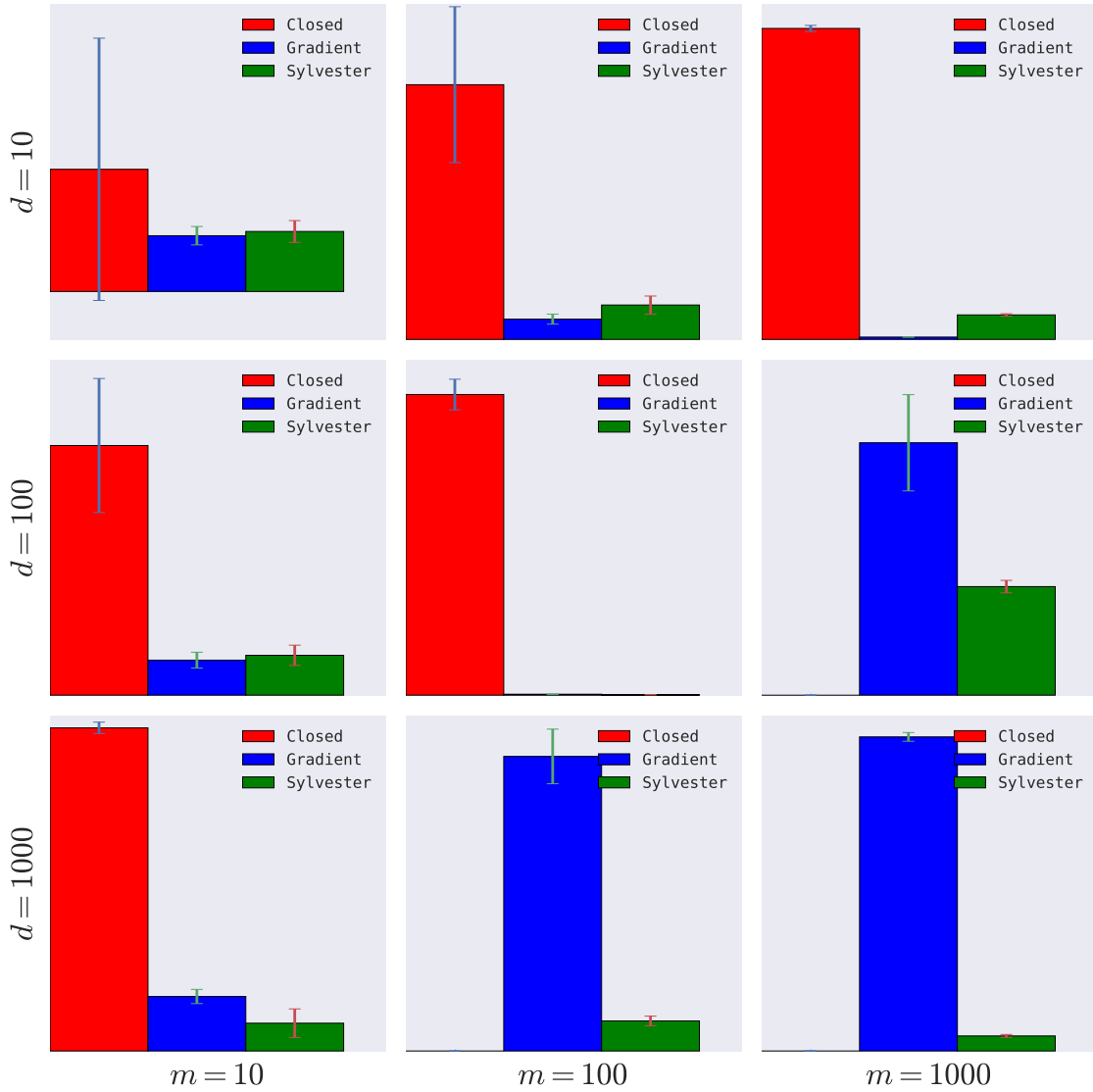


Figure 1: Each experiment is repeated 10 times. We plot the mean run time (seconds) and the standard deviation for each algorithm under each experimental configuration. Closed form solution does not scale when $md \geq 10^4$.

$y_2 = 0$, and $y_3 = -8x_1 - 8x_2 - 8$. The outputs of those regression functions are corrupted by Gaussian noise with mean 0 and variance 1. The true weight matrix is given by

$$W^* = \begin{pmatrix} 10 & 0 & -8 \\ 10 & 0 & -8 \end{pmatrix}$$

For this problem, the first row of W^* corresponds to the weight vector of the feature x_1 across the tasks and the second row corresponds to the weight vector of x_2 . Each column represents a task vector. Hence we expect that the correlation between x_1 and x_2 is 1.0, and we also expect that the

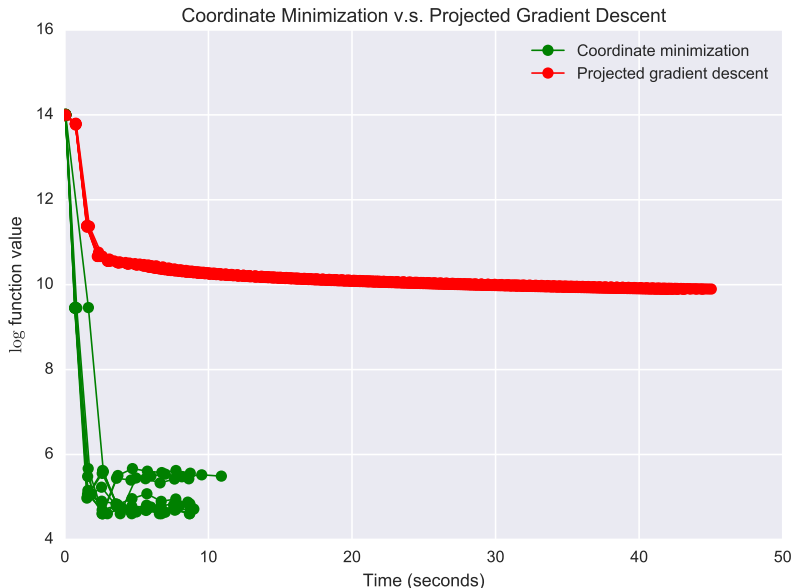


Figure 2: The convergence speed of coordinate minimization versus projected gradient descent. All the experiments are repeated for 10 times.

correlation between the first and the third task to be -1.0 while the correlations for the other two pairs of tasks are 0.0. We apply FETR to this problem, setting $\eta, \rho = 10^{-3}$, $l = 10^{-3}$ and $u = 10^3$. After the algorithm converges, the estimated regression functions are $\hat{y}_1 = 10.00x_1 + 9.99x_2 + 9.43$, $\hat{y}_2 = 0.00$ and $\hat{y}_3 = -7.99x_1 - 8.01x_2 - 7.56$, with the following feature and task correlation matrices (after normalization):

$$\Omega_1 = \begin{pmatrix} 1.00 & 0.99 \\ 0.99 & 1.00 \end{pmatrix}, \quad \Omega_2 = \begin{pmatrix} 1.00 & 0.00 & -1.01 \\ 0.00 & 1.00 & 0.00 \\ -1.01 & 0.00 & 1.00 \end{pmatrix}$$

This synthetic experiment shows that both the learned feature correlation matrix and task correlation matrix conform to our expectation, demonstrating the effectiveness of FETR on this synthetic problem.

4.3 Robot Inverse Dynamics

We evaluate FETR against other multi-task learning algorithms on the inverse dynamics problem for a seven degree-of-freedom (DOF) SARCOS anthropomorphic robot arm.² The goal of this task is to map from a 21-dimensional input space (7 joint positions, 7 joint velocities, 7 joint accelerations) to the corresponding 7 joint torques. Hence there are 7 tasks and the inputs are shared among all the tasks. The training set and test set contain 44,484 and 4,449 examples, respectively. We further partition the training set into a development set and a validation set, which contain 31,138 and 13,346 instances. We use the validation set to do the model selection. Specifically, we train multiple models on the development set with different configurations of hyperparameters ranging

2. <http://www.gaussianprocess.org/gpml/data/>

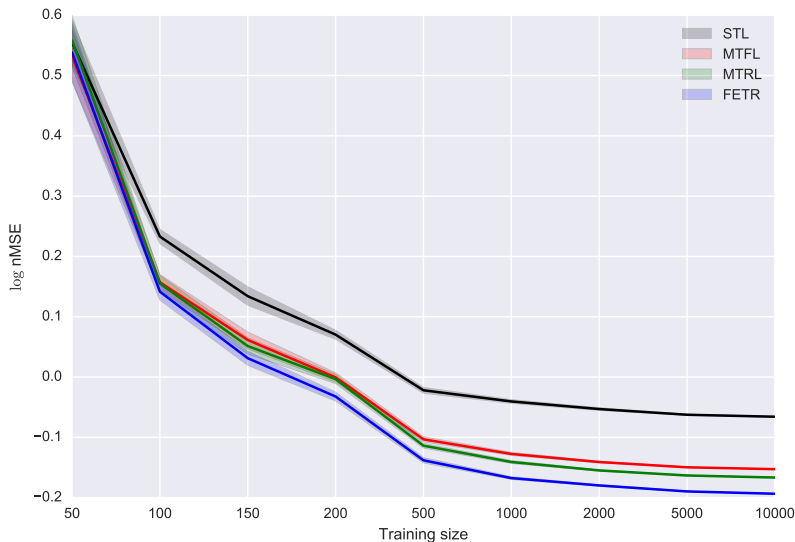


Figure 3: The log total normalized mean squared error of 7 tasks on the SARCOS data set. The x -axis represents the size of the training data set.

from $\eta = \{10^{-5}, \dots, 10^2\}$ and $\rho = \{10^{-5}, \dots, 10^2\}$, and for each model we select the one with the best mean-squared error (MSE) on the validation set. In all the experiments we fix $l = 10^{-3}$ and $u = 10^3$ as we observe the results are not very sensitive to these hyperparameters.

We compare FETR with multi-task feature learning (Evgeniou and Pontil, 2007) (MTFL) and multi-task relationship learning (Zhang and Yeung, 2010a) (MTRL), which can be treated as two different special cases of our model. To have a more controlled, fair comparison between all the methods, we implement both MTFL and MTRL, and use the same experimental setting, including model selection, as FETR. For each task, we use ridge regression as our baseline model, and denote it as single task learning (STL). For each method, the best model on the validation set is used to do prediction, and we report its MSE score on the test set for each task. The smaller the MSE score, the better the predictive result. The results are summarized in Table 1. As expected, when the size of the training data set is large, all the multi-task learning methods perform at least as well as the baseline STL method.

Table 1: Mean squared error of different methods on the SARCOS data. Each column corresponds to one task.

Method	1st DOF	2nd DOF	3rd DOF	4th DOF	5th DOF	6th DOF	7th DOF
STL	31.40	22.90	9.13	10.30	0.14	0.84	0.46
MTFL	31.41	22.91	9.13	10.33	0.14	0.83	0.45
MTRL	31.09	22.69	9.08	9.74	0.14	0.83	0.44
FETR	31.08	22.68	9.08	9.73	0.13	0.83	0.43

Among the three multi-task learning methods, FETR achieves the lowest test set mean square error. FETR can learn both covariance matrices over features and tasks simultaneously, while the other two methods can only estimate one of them. To illustrate this, we show the covariance matrices

estimated by MTFE, MTRL and FETR in the appendix. We also test the performance of all four methods as the size of the training set increases. In order to summarize an overall performance score for better visualization, we use the log total normalized mean squared error of seven tasks on the original test data set, that is, the log sum of the mean squared error divided by the variance of the ground truth. This helps to illustrate the advantages of multi-task learning methods over single task learning as the data set gets larger. For each training set size, we repeat the experiments 10 times, by randomly sampling a subset of the corresponding size from the whole training set. We depict the mean log nMSE of all four methods as well as the standard deviation in Fig. 3.

We also plot the covariance matrices estimated by MTFE, MTRL and FETR to compare the correlation structures found by these algorithms; see Fig. 4. It is worth mentioning that not only does FETR learn both correlation matrices, but it also detects more correlations between features than MTFE. For example, the task correlation matrix learned by FETR exhibits a block diagonal structure, meaning that the weight vectors for the first 4 tasks are roughly uncorrelated. Such pattern is not shown in the task correlation matrix learned by MTRL. On the other hand, FETR detects more correlations among features than MTFE, as shown in Fig. 4.

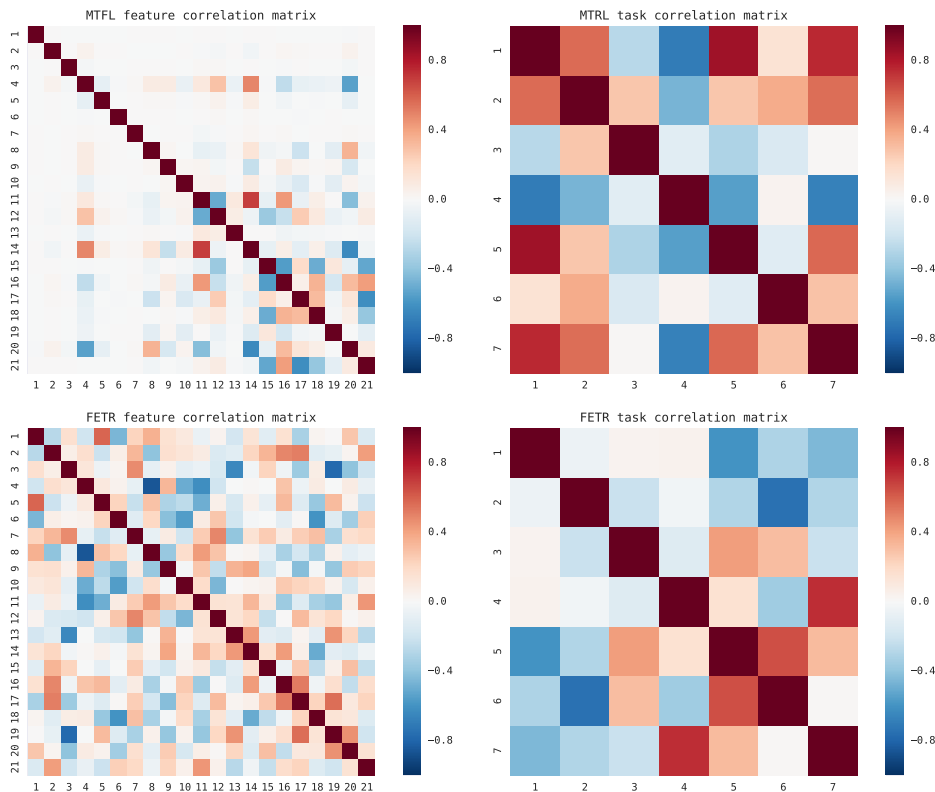


Figure 4: Correlation matrices of feature vectors and task vectors learned by MTFE, MTRL and FETR.

5. Related Work

Multi-task learning is an area of active research in machine learning and has received a lot of attention in the past years (Thrun, 1996b; Caruana, 1997; Yu et al., 2005; Bonilla et al., 2007a,b; Argyriou et al., 2007, 2008; Zhang and Yeung, 2010a). Research on multi-task learning has been carried in several strands. Early work focuses on sharing knowledge in separate tasks by sharing hidden representations, for example, hidden layer of units in neural networks (Caruana, 1997). Another stream of works constructs a Gaussian process prior over the regression functions in different tasks and the transfer of knowledge between tasks is enforced by the structure of the covariance functions/kernels of the Gaussian process prior. Bonilla et al. (2007a) presents a kernel multi-task learning approach with Gaussian process prior where task-specific features are assumed to be available. They concatenate the feature for input instance with the task feature and then define a kernel covariance function over the regression functions among different tasks. The learning is reduced to inferring the hyperparameters of the kernel function by maximizing the marginal log-likelihood of the instances by either EM or gradient ascent. This approach essentially decomposes the joint kernel function over regression functions into two separate kernels: one measures the similarity among tasks and the other measures the similarity among instances. A closely related approach in this strand is to consider a nonparametric kernel matrix over the tasks rather than a parametrized kernel function (Bonilla et al., 2007b). However, the kernel over input instances is still restricted to be parametrized in order to avoid the expensive computation of semidefinite programming over input features. In contrast, FETR optimizes both of the feature and task covariance matrices directly without assumption about their parametrized forms.

Argyriou et al. (2008) and (Zhang and Yeung, 2010a) develop MTFL and MTRL, which can be viewed as convex frameworks of learning the feature and the task-relatedness covariance matrices, respectively. Both MTFL and MTRL are essentially convex regularization methods that exploit the feature and task relatedness by imposing trace constraints on W after proper transformations. Covariance matrices in MTFL and MTRL are not restricted to have specific parametrized forms, and from this perspective, (Evgeniou et al., 2005; Evgeniou and Pontil, 2004; Kato et al., 2008) can be understood as special cases of MTFL and MTRL where the covariance matrices are constrained to be (weighted) graph Laplacians. However, in MTFL only the feature covariance matrix is being optimized and the task-relatedness covariance matrix is assumed to be the identity, while in MTRL only the task-relatedness covariance matrix is being optimized and the feature covariance matrix is, again, assumed to be the identity. We take inspiration from these two previous works and propose a general regularization framework, FETR, that models and optimizes both task and feature relationships directly. It is worth emphasizing here that both MTFL and MTRL can be treated as special cases of FETR where one of the two covariance matrices are assumed to be the identity, which corresponds to left/right spherical matrix normal distributions. The objective function of FETR is not convex, but multi-convex. Efficient coordinate-wise minimization algorithm with closed form solutions for each subproblem is designed to tackle the multi-convex objective in FETR.

Perhaps the most related work to FETR is Zhang and Schneider (2010). Both that work and our approach consider a multi-task learning framework where both the task and feature covariance matrices are inferred from data. However, while the authors make a sparsity assumption on the two covariance matrices, our approach is more general in the sense that we are free of this assumption. Secondly and more importantly, while in that work the optimization w.r.t the two covariance matrices employs an iterative method (either proximal method or coordinate descent) to approximate

the optimal solution, we obtain an efficient, non-iterative solution by reduction to a graph matching problem. Note that in order to optimize the covariance matrix using our method, one SVD is enough, while in Zhang et al. each iteration requires an SVD. This makes our approach computationally more efficient than the one used in Zhang and Schneider (2010), and statistically our approach makes less assumption than the framework proposed in Zhang and Schneider (2010).

6. Discussion and future work

We develop a multi-convex framework for multi-task learning that improves predictions by learning relationships both between tasks and between features. Our framework is a generalization of related approaches in multi-task learning, that either learn task relationships, or feature relationships. We develop a multi-convex formulation of the problem, as well as an algorithm for block coordinate-wise minimization. By using the theory of doubly stochastic matrices, we are able to reduce the underlying matrix optimization subproblem into a minimum weight perfect matching problem on a complete bipartite graph, and solve it in closed form. Our method is orders of magnitude faster than an off-the-shelf projected gradient descent method, and it shows improved performance on synthetic datasets as well as on a real-world dataset for robotic modeling. While the current paper discusses our approach in the context of linear regression, it can be extended to other types of prediction tasks, such as logistic regression, linear SVM, etc.

References

- A. Argyriou, M. Pontil, Y. Ying, and C. A. Micchelli. A spectral regularization framework for multi-task structure learning. In *Advances in neural information processing systems*, 2007.
- A. Argyriou, T. Evgeniou, and M. Pontil. Convex multi-task feature learning. *Machine Learning*, 73(3):243–272, 2008.
- R. H. Bartels and G. Stewart. Solution of the matrix equation $AX + XB = C$ [F4]. *Communications of the ACM*, 15(9):820–826, 1972.
- D. Bertsimas and J. N. Tsitsiklis. *Introduction to linear optimization*, volume 6. Athena Scientific Belmont, MA, 1997.
- R. Bhatia and P. Rosenthal. How and why to solve the operator equation $ax - xb = y$. *Bulletin of the London Mathematical Society*, 29(01):1–21, 1997.
- E. V. Bonilla, F. V. Agakov, and C. Williams. Kernel multi-task learning using task-specific features. In *International Conference on Artificial Intelligence and Statistics*, pages 43–50, 2007a.
- E. V. Bonilla, K. M. Chai, and C. Williams. Multi-task gaussian process prediction. In *Advances in neural information processing systems*, pages 153–160, 2007b.
- S. Boyd and L. Vandenberghe. *Convex optimization*. 2004.
- B. P. Carlin and T. A. Louis. Bayes and empirical bayes methods for data analysis. *Statistics and Computing*, 7(2):153–154, 1997.
- R. Caruana. Multitask learning. *Machine learning*, 28(1):41–75, 1997.

- F. Dufossé and B. Uçar. Notes on birkhoff–von neumann decomposition of doubly stochastic matrices. *Linear Algebra and its Applications*, 497:108–115, 2016.
- A. Evgeniou and M. Pontil. Multi-task feature learning. *Advances in neural information processing systems*, 19:41, 2007.
- T. Evgeniou and M. Pontil. Regularized multi–task learning. In *Proceedings of the tenth ACM SIGKDD international conference on Knowledge discovery and data mining*, pages 109–117. ACM, 2004.
- T. Evgeniou, C. A. Micchelli, and M. Pontil. Learning multiple tasks with kernel methods. In *Journal of Machine Learning Research*, pages 615–637, 2005.
- J. Gorski, F. Pfeuffer, and K. Klamroth. Biconvex sets and optimization with biconvex functions: a survey and extensions. *Mathematical Methods of Operations Research*, 2007.
- A. K. Gupta and D. K. Nagar. *Matrix variate distributions*, volume 104. CRC Press, 1999.
- T. Kato, H. Kashima, M. Sugiyama, and K. Asai. Multi-task learning via conic programming. In *Advances in Neural Information Processing Systems*, pages 737–744, 2008.
- Y. Li, X. Tian, T. Liu, and D. Tao. Multi-task model and feature joint learning. In *Proceedings of the 24th International Conference on Artificial Intelligence*, pages 3643–3649. AAAI Press, 2015.
- J. Liu, S. Ji, and J. Ye. Multi-task feature learning via efficient l_2, l_1 -norm minimization. In *Proceedings of the twenty-fifth conference on uncertainty in artificial intelligence*, pages 339–348. AUAI Press, 2009.
- Y. Nesterov. *Introductory lectures on convex optimization: A basic course*, volume 87. Springer Science & Business Media, 2013.
- J. R. Shewchuk et al. An introduction to the conjugate gradient method without the agonizing pain, 1994.
- S. Thrun. Explanation-based neural network learning. In *Explanation-Based Neural Network Learning*, pages 19–48. Springer, 1996a.
- S. Thrun. Is earning the n-th thing any easier than learning the first? *Advances in neural information processing systems*, pages 640–646, 1996b.
- Y. Xu and W. Yin. A block coordinate descent method for regularized multiconvex optimization with applications to nonnegative tensor factorization and completion. *SIAM Journal on imaging sciences*, 2013.
- K. Yu, V. Tresp, and A. Schwaighofer. Learning gaussian processes from multiple tasks. In *Proceedings of the 22nd international conference on Machine learning*, pages 1012–1019. ACM, 2005.
- Y. Zhang and J. G. Schneider. Learning multiple tasks with a sparse matrix-normal penalty. In *Advances in Neural Information Processing Systems*, pages 2550–2558, 2010.

- Y. Zhang and D.-Y. Yeung. A convex formulation for learning task relationships in multi-task learning. 2010a.
- Y. Zhang and D.-Y. Yeung. Multi-task learning using generalized t process. In *AISTATS*, pages 964–971, 2010b.

Appendix A. Proofs

A.1 Proofs of Claim 3.1

Claim 3.1. The objective function in (6) is multi-convex.

Proof. First, it is straightforward to check that the constraint set $lI_d \preceq \Sigma_1 \preceq uI_d$ and $lI_m \preceq \Sigma_2 \preceq uI_m$ are convex. For any fixed Σ_1 and Σ_2 , the objective function in terms of W can be expressed as

$$\sum_{i=1}^m \left(\sum_{j=1}^{n_i} (y_i^j - \mathbf{w}_i^T \mathbf{x}_i^j)^2 + \eta \|\mathbf{w}_i\|_2^2 \right) + \rho \text{tr}(\Sigma_1 W \Sigma_2 W^T)$$

The first term decomposes over tasks and for each task vector \mathbf{w}_i , $\sum_{j=1}^{n_i} (y_i^j - \mathbf{w}_i^T \mathbf{x}_i^j)^2 + \eta \|\mathbf{w}_i\|_2^2$ is a quadratic function for each \mathbf{w}_i , so the summation is also convex in W . Since $\Sigma_1 \in \mathbb{S}_+^d$ and $\Sigma_2 \in \mathbb{S}_+^m$, we can further rewrite the second term above as

$$\rho \text{tr}(\Sigma_1 W \Sigma_2 W^T) = \rho \text{tr}((\Sigma_1^{1/2} W \Sigma_2^{1/2})(\Sigma_1^{1/2} W \Sigma_2^{1/2})^T) = \rho \|\Sigma_1^{1/2} W \Sigma_2^{1/2}\|_F^2$$

This is the Frobenius norm of the matrix $\Sigma_1^{1/2} W \Sigma_2^{1/2}$, which is a linear transformation of W when both Σ_1 and Σ_2 are fixed, hence this is also a convex function of W . Overall the objective function with respect to W when both Ω_1 and Ω_2 are fixed is convex. For any fixed W and Σ_2 , consider the objective function with respect to Σ_1 :

$$-\rho m \log |\Sigma_1| + \rho \text{tr}(\Sigma_1 C)$$

where $C = W \Sigma_2 W^T$ is a constant matrix. Since $\log |\Sigma_1|$ is concave in Σ_1 and $\text{tr}(\Sigma_1 C)$ is a linear function of Σ_1 , it directly follows that $-\rho m \log |\Sigma_1| + \rho \text{tr}(\Sigma_1 C)$ is a convex function of Σ_1 . A similar argument can be applied to Σ_2 as well. \blacksquare

A.2 Proof of Claim 3.2

Claim 3.2. (8) can be solved in closed form in $O(m^3 d^3 + m n d^2)$ time; the optimal $\text{vec}(W^*)$ has the following form:

$$(I_m \otimes (X^T X) + \eta I_{md} + \rho \Sigma_2 \otimes \Sigma_1)^{-1} \text{vec}(X^T Y) \quad (10)$$

To prove this claim, we need the following facts about tensor product:

Fact A.1. Let A be a matrix. Then $\|A\|_F = \|\text{vec}(A)\|_2$.

Fact A.2. Let $A \in \mathbb{R}^{m_1 \times n_1}$, $B \in \mathbb{R}^{n_1 \times n_2}$ and $C \in \mathbb{R}^{n_2 \times m_2}$. Then $\text{vec}(ABC) = (C^T \otimes A) \text{vec}(B)$.

Fact A.3. Let $S_1 \in \mathbb{R}^{m_1 \times n_1}$, $S_2 \in \mathbb{R}^{n_1 \times p_1}$ and $T_1 \in \mathbb{R}^{m_2 \times n_2}$, $T_2 \in \mathbb{R}^{n_2 \times p_2}$. Then $(S_1 \otimes S_2)(T_1 \otimes T_2) = (S_1 S_2) \otimes (T_1 T_2)$.

Fact A.4. Let $A \in \mathbb{R}^{n \times n}$ and $B \in \mathbb{R}^{m \times m}$. Let $\{\mu_1, \dots, \mu_n\}$ be the spectrum of A and $\{\nu_1, \dots, \nu_m\}$ be the spectrum of B . Then the spectrum of $A \otimes B$ is $\{\mu_i \nu_j : 1 \leq i \leq n, 1 \leq j \leq m\}$.

we can show the following result by transforming W into its isomorphic counterpart:

Proof.

$$\begin{aligned}
 & \|Y - XW\|_F^2 + \eta\|W\|_F^2 + \rho\|\Sigma_1^{1/2}W\Sigma_2^{1/2}\|_F^2 \\
 = & \|\text{vec}(Y - XW)\|_2^2 + \eta\|\text{vec}(W)\|_2^2 + \rho\|\text{vec}(\Sigma_1^{1/2}W\Sigma_2^{1/2})\|_2^2 && \text{(By Fact A.1)} \\
 = & \|\text{vec}(Y) - (I_m \otimes X)\text{vec}(W)\|_2^2 + \eta\|\text{vec}(W)\|_2^2 + \rho\|(\Sigma_2^{1/2} \otimes \Sigma_1^{1/2})\text{vec}(W)\|_2^2 && \text{(By Fact A.2)} \\
 = & \text{vec}(W)^T \left((I_m \otimes X)^T(I_m \otimes X) + \eta I_{md} + \rho(\Sigma_2^{1/2} \otimes \Sigma_1^{1/2})^T(\Sigma_2^{1/2} \otimes \Sigma_1^{1/2}) \right) \text{vec}(W) \\
 & - 2\text{vec}(W)^T(I_m \otimes X^T)\text{vec}(Y) + \text{vec}(Y)^T\text{vec}(Y) \\
 = & \text{vec}(W)^T \left((I_m \otimes X^T X) + \eta I_{md} + \rho(\Sigma_2 \otimes \Sigma_1) \right) \text{vec}(W) \\
 & - 2\text{vec}(W)^T(I_m \otimes X^T)\text{vec}(Y) + \text{vec}(Y)^T\text{vec}(Y) && \text{(By Fact A.3)}
 \end{aligned}$$

The last equation above is a quadratic function of $\text{vec}(W)$, from which we can read off that the optimal solution W^* should satisfy:

$$\text{vec}(W^*) = (I_m \otimes (X^T X) + \eta I_{md} + \rho \Sigma_2 \otimes \Sigma_1)^{-1} \text{vec}(X^T Y) \quad (21)$$

W^* can then be obtained simply by reformatting $\text{vec}(W^*)$ into a $d \times m$ matrix. The computational bottleneck in the above procedure is in solving an $md \times md$ system of equations, which scales as $O(m^3 d^3)$ if no further structure is available. The overall computational complexity is $O(m^3 d^3 + mnd^2)$. \blacksquare

A.3 Proof of Thm. 3.1

To analyze the convergence rate of gradient descent in this case, we start by bounding the smallest and largest eigenvalue of the quadratic system shown in Eq. 21.

Lemma A.1 (Weyl's inequality). Let A, B and C be n -by- n Hermitian matrices, and $C = A + B$. Let $a_1 \geq \dots \geq a_n, b_1 \geq \dots \geq b_n$ and $c_1 \geq \dots \geq c_n$ be the eigenvalues of A, B and C respectively. Then the following inequalities hold for $r + s - 1 \leq i \leq j + k - n, \forall i = 1, \dots, n$:

$$a_j + b_k \leq c_i \leq a_r + b_s$$

Let $\lambda_k(A)$ be the k -th largest eigenvalue of matrix A .

Lemma A.2. If Σ_1 and Σ_2 are feasible in (7), then

$$\begin{aligned}
 \lambda_1(I_m \otimes (X^T X) + \eta I_{md} + \rho \Sigma_2 \otimes \Sigma_1) &\leq \lambda_1(X^T X) + \eta + \rho u^2 \\
 \lambda_{md}(I_m \otimes (X^T X) + \eta I_{md} + \rho \Sigma_2 \otimes \Sigma_1) &\geq \lambda_d(X^T X) + \eta + \rho l^2
 \end{aligned}$$

Proof. By Weyl's inequality, setting $r = s = i = 1$, we have $c_1 \leq a_1 + b_1$. Set $j = k = i = n$, we have $c_n \geq a_n + b_n$. We can bound the largest and smallest eigenvalues of $I_m \otimes (X^T X) + \eta I_{md} + \rho \Sigma_2 \otimes \Sigma_1$ as follows:

$$\begin{aligned}
 & \lambda_1(I_m \otimes (X^T X) + \eta I_{md} + \rho \Sigma_2 \otimes \Sigma_1) \\
 \leq & \lambda_1(I_m \otimes (X^T X)) + \lambda_1(\eta I_{md}) + \lambda_1(\rho \Sigma_2 \otimes \Sigma_1) && \text{(By Weyl's inequality)} \\
 = & \lambda_1(I_m)\lambda_1(X^T X) + \eta + \rho\lambda_1(\Sigma_1)\lambda_1(\Sigma_2) && \text{(By Fact A.4)} \\
 \leq & \lambda_1(X^T X) + \eta + \rho u^2 && \text{(By the feasibility assumption)}
 \end{aligned}$$

and

$$\begin{aligned}
 & \lambda_{md}(I_m \otimes (X^T X) + \eta I_{md} + \rho \Sigma_2 \otimes \Sigma_1) \\
 \geq & \lambda_{md}(I_m \otimes (X^T X)) + \lambda_{md}(\eta I_{md}) + \lambda_{md}(\rho \Sigma_2 \otimes \Sigma_1) && \text{(By Weyl's inequality)} \\
 = & \lambda_m(I_m) \lambda_d(X^T X) + \eta + \rho \lambda_m(\Sigma_1) \lambda_d(\Sigma_2) && \text{(By Fact A.4)} \\
 \geq & \lambda_d(X^T X) + \eta + \rho l^2 && \text{(By the feasibility assumption)}
 \end{aligned}$$

■

We will first prove the following two lemmas using the fact that the spectral norm of the Hessian matrix $\nabla^2 h(W)$ is bounded.

Lemma A.3. Let $f(W) : \mathbb{R}^{d \times m} \mapsto \mathbb{R}$ be a twice differentiable function with $\lambda_1(\nabla^2 f(W)) \leq L$. $L > 0$ is a constant. The minimum value of $f(W)$ can be achieved. Let $W^* = \arg \min_W f(W)$, then

$$f(W^*) \leq f(W) - \frac{1}{2L} \|\nabla f(W)\|_F^2$$

Proof. Since $f(W)$ is twice differentiable with $\lambda_1(\nabla^2 f(W)) \leq L$, by the Lagrangian mean value theorem, $\forall W, \widetilde{W}$, we can find a value $0 < t(W, \widetilde{W}) < 1$, such that

$$\begin{aligned}
 f(\widetilde{W}) &= f(W) + \text{tr}(\nabla f(W)^T (\widetilde{W} - W)) + \frac{1}{2} \text{vec}(\widetilde{W} - W)^T \nabla^2 f(tW + (1-t)\widetilde{W}) \text{vec}(\widetilde{W} - W) \\
 &\leq f(W) + \text{tr}(\nabla f(W)^T (\widetilde{W} - W)) + \frac{L}{2} \|\widetilde{W} - W\|_F^2
 \end{aligned}$$

Since W^* achieves the minimum value of $f(W)$, we can use the above result to obtain:

$$\begin{aligned}
 f(W^*) &= \inf_{\widetilde{W}} f(\widetilde{W}) \\
 &\leq \inf_{\widetilde{W}} f(W) + \text{tr}(\nabla f(W)^T (\widetilde{W} - W)) + \frac{L}{2} \|\widetilde{W} - W\|_F^2 \\
 &= f(W) - \frac{1}{2L} \|\nabla f(W)\|_F^2
 \end{aligned}$$

where the last equation comes from the fact that the minimum of a quadratic function with respect to \widetilde{W} can be achieved at $\widetilde{W} = W - \frac{1}{L} \nabla f(W)$. ■

Lemma A.4. Let $f(W) : \mathbb{R}^{d \times m} \mapsto \mathbb{R}$ be a convex, twice differentiable function with $\lambda_1(\nabla^2 f(W)) \leq L$. $L > 0$ is a constant, then $\forall W_1, W_2$:

$$\text{tr}((\nabla f(W_1) - \nabla f(W_2))^T (W_1 - W_2)) \geq \frac{1}{L} \|\nabla f(W_1) - \nabla f(W_2)\|_F^2$$

Proof. For all W_1, W_2 , we can construct the following two functions:

$$f_{W_1}(Z) = f(Z) - \text{tr}(\nabla f(W_1)^T Z), \quad f_{W_2}(Z) = f(Z) - \text{tr}(\nabla f(W_2)^T Z)$$

Since $f(W)$ is a convex, twice differentiable function with respect to W , it follows that both $f_{W_1}(Z)$ and $f_{W_2}(Z)$ are convex, twice differentiable functions with respect to Z . The first-order optimality condition of convex functions gives the following conditions to hold for Z which achieves the optimality:

$$\nabla f_{W_1}(Z) = \nabla f(Z) - \nabla f(W_1) = 0, \quad \nabla f_{W_2}(Z) = \nabla f(Z) - \nabla f(W_2) = 0$$

Plug in W_1 and W_2 into the above optimality conditions respectively. From the first-order optimality condition we know that W_1 and W_2 achieves the optimal solutions of $f_{W_1}(Z)$ and $f_{W_2}(Z)$, respectively.

Now applying Lemma A.3 to $f_{W_1}(Z)$ and $f_{W_2}(Z)$, we have:

$$((W_2) - \text{tr}(\nabla f(W_1)^T W_2)) - ((W_1) - \text{tr}(\nabla f(W_1)^T W_1)) \geq \frac{1}{2L} \|\nabla f(W_1) - \nabla f(W_2)\|_F^2$$

$$((W_1) - \text{tr}(\nabla f(W_2)^T W_1)) - ((W_2) - \text{tr}(\nabla f(W_2)^T W_2)) \geq \frac{1}{2L} \|\nabla f(W_1) - \nabla f(W_2)\|_F^2$$

Adding the above two equations leads to

$$\text{tr}((\nabla f(W_1) - \nabla f(W_2))^T (W_1 - W_2)) \geq \frac{1}{L} \|\nabla f(W_1) - \nabla f(W_2)\|_F^2$$

■

We can now proceed to show Thm. 3.1.

Theorem 3.1. Let $\lambda_l = \lambda_d(X^T X) + \eta + \rho l^2$, $\lambda_u = \lambda_1(X^T X) + \eta + \rho u^2$ and $\gamma = (\frac{\lambda_u - \lambda_l}{\lambda_u + \lambda_l})^2$. Choose $0 < t \leq 2/(\lambda_u + \lambda_l)$. For all $\varepsilon > 0$, gradient descent with step size t converges to the optimal solution within $O(\log_{1/\gamma}(1/\varepsilon))$ steps.

Proof. Define function $g(W)$ as follows:

$$g(W) = h(W) - \frac{\lambda_l}{2} \|W\|_F^2$$

Since we have already bounded that $\lambda_{md}(\nabla^2 h(W)) \geq \lambda_l$, it follows that $g(W)$ is a convex function and furthermore $\lambda_1(\nabla^2 g(W)) \leq \lambda_u - \lambda_l$. Applying Lemma A.4 to g , $\forall W_1, W_2 \in \mathbb{R}^{d \times m}$, we have:

$$\text{tr}((\nabla g(W_1) - \nabla g(W_2))^T (W_1 - W_2)) \geq \frac{1}{\lambda_u - \lambda_l} \|\nabla g(W_1) - \nabla g(W_2)\|_F^2$$

Plug in $\nabla g(W) = \nabla h(W) - \lambda_l W$ into the above inequality and after some algebraic manipulations, we have:

$$\text{tr}((\nabla h(W_1) - \nabla h(W_2))^T (W_1 - W_2)) \geq \frac{1}{\lambda_u + \lambda_l} \|\nabla h(W_1) - \nabla h(W_2)\|_F^2 + \frac{\lambda_u \lambda_l}{\lambda_u + \lambda_l} \|W_1 - W_2\|_F^2 \quad (22)$$

Let $W^* = \arg \min_W h(W)$. Within each iteration of Alg. 3, we have the update formula as $W^+ = W - t\nabla h(W)$, we can bound $\|W^+ - W^*\|_F^2$ as follows

$$\begin{aligned}
 \|W^+ - W^*\|_F^2 &= \|W - W^* - t\nabla h(W)\|_F^2 \\
 &= \|W - W^*\|_F^2 + t^2 \|\nabla h(W)\|_F^2 - 2t \text{tr}((W - W^*)^T \nabla h(W)) \\
 &\leq (1 - 2t \frac{\lambda_u \lambda_l}{\lambda_u + \lambda_l}) \|W - W^*\|_F^2 + t(t - \frac{2}{\lambda_u + \lambda_l}) \|\nabla h(W)\|_F^2 \quad (\text{By inequality 22}) \\
 &\leq (1 - 2t \frac{\lambda_u \lambda_l}{\lambda_u + \lambda_l}) \|W - W^*\|_F^2 \quad (\text{For } 0 < t \leq 2/(\lambda_u + \lambda_l))
 \end{aligned}$$

Apply the above inequality recursively for T times, we have

$$\|W^{(T)} - W^*\|_F^2 \leq \gamma^T \|W^{(0)} - W^*\|_F^2$$

where $\gamma = 1 - 2t \frac{\lambda_u \lambda_l}{\lambda_u + \lambda_l}$. For $t = 2/(\lambda_u + \lambda_l)$, we have

$$\gamma = 1 - 4\lambda_u \lambda_l / (\lambda_l + \lambda_u)^2 = \left(\frac{\lambda_u - \lambda_l}{\lambda_u + \lambda_l} \right)^2$$

Now pick $\forall \varepsilon > 0$, setting the upper bound $\gamma^T \|W^{(0)} - W^*\|_F^2 \leq \varepsilon$ and solve for T , we have

$$T \geq \log_{1/\gamma}(C/\varepsilon) = O(\log_{1/\gamma}(1/\varepsilon))$$

where $C = \|W^{(0)} - W^*\|_F^2$ is a constant. ■

The pseudocode of the gradient descent is shown in Alg. 3.

Algorithm 3 Gradient descent with fixed step-size.

Input: Initial W , X , Y and approximation accuracy ε .

- 1: $\lambda_u \leftarrow \lambda_1(X^T X) + \eta + \rho u^2$.
 - 2: $\lambda_l \leftarrow \lambda_d(X^T X) + \eta + \rho l^2$.
 - 3: **Step size** $t \leftarrow 2/(\lambda_l + \lambda_u)$.
 - 4: **while** $\|\nabla h(W)\|_F > \varepsilon$ **do**
 - 5: $W \leftarrow W - t(X^T(Y - XW) + \eta W + \rho \Sigma_1 W \Sigma_2)$.
 - 6: **end while**
-

A.4 Proof of Lemma 3.1

Lemma 3.1. There exists an optimal solution P to the optimization problem (18) that is a $d \times d$ permutation matrix.

Proof. Note that the optimization problem (18) in terms of P is a linear program with the Birkhoff polytope being the feasible region. It follows from Thm. 3.2 and Thm. 3.3 that at least one optimal solution P is an $d \times d$ permutation matrix. ■

A.5 Proof of Thm. 3.4

Theorem 3.4. The minimum value of (18) is equal to the minimum weight of a perfect matching on $G = (V_\lambda, V_\nu, E, w)$. Furthermore, the optimal solution P of (18) can be constructed from the minimum-weight perfect matching M on G .

Proof. By Lemma 3.1, the optimal value is achieved when P is a permutation matrix. Given a permutation matrix P , we can understand P as a bijective mapping from the index of rows to the index of columns. Specifically, construct a permutation $\pi_P : [d] \rightarrow [d]$ from P as follows. For each row index $i \in [d]$, $\pi_P(i) = j$ iff $P_{ij} = 1$. It follows that π_P is a permutation of $[d]$ since P is assumed to be a permutation matrix. The objective function in (18) can be written in terms of π_P as

$$\lambda^T P \nu = \sum_{i=1}^d \lambda_i \nu_{\pi_P(i)}$$

which is exactly the weight of the perfect matching on $G(V_\lambda, V_\nu, E, w)$ given by π_P :

$$w(\pi_P) = w(\{(i, \pi_P(i)) : 1 \leq i \leq d\}) = \sum_{i=1}^d \lambda_i \nu_{\pi_P(i)}$$

Similarly, in the other direction, given any perfect matching $\pi : [d] \rightarrow [d]$ on the bipartite graph $G(V_\lambda, V_\nu, E, w)$, we can construct a corresponding permutation matrix P_π : $P_{\pi,ij} = 1$ iff $\pi(i) = j$, otherwise 0. Since π is a perfect matching, the constructed P_π is guaranteed to be a permutation matrix.

Hence the problem of finding the optimal value of (18) is equivalent to finding the minimum weight perfect matching on the constructed bipartite graph $G(V_\lambda, V_\nu, E, w)$. Note that the above constructive process also shows how to recover the optimal permutation matrix P_{π^*} from the minimum weight perfect matching π^* . ■

A.6 Proof of Thm. 3.5

Note that $\lambda = (\lambda_1, \dots, \lambda_d)$ and $\nu = (\nu_1, \dots, \nu_d)$ are assumed to satisfy $\lambda_1 \geq \dots \geq \lambda_d$ and $\nu_1 \leq \dots \leq \nu_d$. To make the discussion more clear, we first make the following definition of an *inverse pair*.

Definition A.1 (Inverse pair). Given a perfect match π of $G(V_\lambda, V_\nu, E, w)$, $(\lambda_i, \lambda_j, \nu_k, \nu_l)$ is called an *inverse pair* if $i \leq j, k \leq l$ and $(v_{\lambda_i}, v_{\nu_l}) \in \pi, (v_{\lambda_j}, v_{\nu_k}) \in \pi$.

Lemma A.5. Given a perfect match π of $G(V_\lambda, V_\nu, E, w)$ and assuming π contains an inverse pair $(\lambda_i, \lambda_j, \nu_k, \nu_l)$. Construct $\pi' = \pi \setminus \{(v_{\lambda_i}, v_{\nu_l}), (v_{\lambda_j}, v_{\nu_k})\} \cup \{(v_{\lambda_i}, v_{\nu_k}), (v_{\lambda_j}, v_{\nu_l})\}$. Then $w(\pi') \leq w(\pi)$.

Proof. Let us compare the weights of π and π' . Note that since $i \leq j, k \leq l$, we have $\lambda_i \geq \lambda_j$ and $\nu_k \leq \nu_l$.

$$\begin{aligned} w(\pi') - w(\pi) &= (\lambda_i \nu_k + \lambda_j \nu_l) - (\lambda_i \nu_l + \lambda_j \nu_k) \\ &= (\lambda_i - \lambda_j)(\nu_k - \nu_l) \\ &\leq 0 \end{aligned}$$

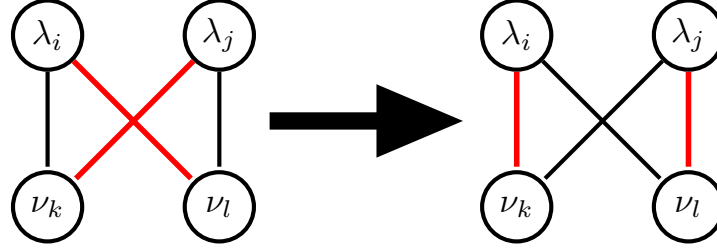


Figure 5: Re-matching an inverse pair $(\lambda_i, \lambda_j, \nu_k, \nu_l) = \{(v_{\lambda_i}, v_{\nu_l}), (v_{\lambda_j}, v_{\nu_k})\}$ on the left side to a match with smaller weight $\{(v_{\lambda_i}, v_{\nu_k}), (v_{\lambda_j}, v_{\nu_l})\}$. Red color is used to highlight edges in the perfect matching.

Intuitively, this lemma says that we can always decrease the weight of a perfect matching by re-matching an inverse pair. Fig. 5 illustrates this process. It is worth emphasizing here that the above re-matching process only involves four nodes, i.e., $v_{\lambda_i}, v_{\nu_l}, v_{\lambda_j}$ and v_{ν_k} . In other words, the other parts of the matching stay unaffected. ■

Using Lemma A.5, we are now ready to prove Thm. 3.5:

Theorem 3.5. Let $\lambda = (\lambda_1, \dots, \lambda_d)$ and $\nu = (\nu_1, \dots, \nu_d)$ with $\lambda_1 \geq \dots \geq \lambda_d$ and $\nu_1 \leq \dots \leq \nu_d$. The minimum-weight perfect matching on G is $\pi^* = \{(v_{\lambda_i}, v_{\nu_i}) : 1 \leq i \leq d\}$ with the minimum weight $w(\pi^*) = \sum_{i=1}^d \lambda_i \nu_i$.

Proof. We will prove by induction.

- **Base case.** The base case is $d = 2$. In this case there are only two valid perfect matchings, i.e., $\{(v_{\lambda_1}, v_{\nu_1}), (v_{\lambda_2}, v_{\nu_2})\}$ or $\{(v_{\lambda_1}, v_{\nu_2}), (v_{\lambda_2}, v_{\nu_1})\}$. Note that the second perfect matching $\{(v_{\lambda_1}, v_{\nu_2}), (v_{\lambda_2}, v_{\nu_1})\}$ is an inverse pair. Hence by Lemma A.5, $w(\{(v_{\lambda_1}, v_{\nu_1}), (v_{\lambda_2}, v_{\nu_2})\}) = \lambda_1 \nu_1 + \lambda_2 \nu_2 \leq \lambda_1 \nu_2 + \lambda_2 \nu_1 = w(\{(v_{\lambda_1}, v_{\nu_2}), (v_{\lambda_2}, v_{\nu_1})\})$.
- **Induction step.** Assume Thm. 3.5 holds for $d = n$. Consider the case when $d = n + 1$. Start from any perfect matching π . Check the matches of node $v_{\lambda_{n+1}}$ and $v_{\nu_{n+1}}$. Here we have two subcases to discuss:
 - If $v_{\lambda_{n+1}}$ is matched to $v_{\nu_{n+1}}$ in π . Then we can remove nodes $v_{\lambda_{n+1}}$ and $v_{\nu_{n+1}}$ from current graph, and this reduces to the case when $n = d$. By induction assumption, the minimum weight perfect matching on the new graph is given by $\sum_{i=1}^n \lambda_i \nu_i$, so the minimum weight on the original graph is $\sum_{i=1}^n \lambda_i \nu_i + \lambda_{n+1} \nu_{n+1} = \sum_{i=1}^{n+1} \lambda_i \nu_i$.
 - If $v_{\lambda_{n+1}}$ is not matched to $v_{\nu_{n+1}}$ in π . Let v_{ν_j} be the match of $v_{\lambda_{n+1}}$ and v_{λ_i} be the match of $v_{\nu_{n+1}}$, where $i \neq n + 1$ and $j \neq n + 1$. In this case we have $i < n + 1$ and $j < n + 1$, so $(\lambda_i, \lambda_{n+1}, \nu_j, \nu_{n+1})$ forms an inverse pair by definition. By Lemma A.5, we can first re-match $v_{\lambda_{n+1}}$ to $v_{\nu_{n+1}}$ and v_{λ_i} to v_{ν_j} to construct a new match π' with $w(\pi') \leq w(\pi)$. In the new matching π' we have the property that $v_{\lambda_{n+1}}$ is matched to $v_{\nu_{n+1}}$, and this becomes the above case that we have already analyzed, so we still have the minimum weight perfect matching to be $\sum_{i=1}^{n+1} \lambda_i \nu_i$.

Intuitively, as shown in Fig. 5, an inverse pair corresponds to a cross in the matching graph. The above inductive proof basically works from right to left to recursively remove inverse pairs (crosses) from the matching graph. Each re-matching step in the proof will decrease the number of inverse pairs at least by one. The whole process stops until there is no inverse pair in the current perfect matching. Since the total number of possible inverse pairs, the above process can stop in finite steps. We illustrate the process of removing inverse pairs in Fig. 6. ■

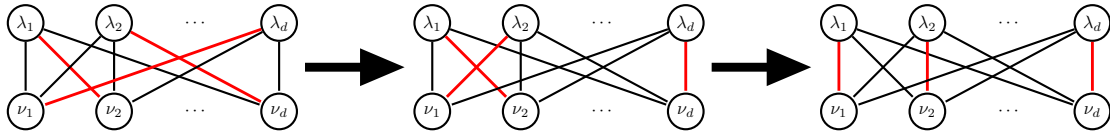


Figure 6: The inductive proof works by recursively removing inverse pairs from the right side of the graph to the left side of the graph. The process stops until there is no inverse pair in the matching. Red color is used to highlight edges in the perfect matching.